Quasinormal modes of a scalar and an electromagnetic field in Finslerian-Schwarzschild spacetime

Xin Li* and Su-Ping Zhao†

Department of Physics, Chongqing University, Chongqing 401331, China

(Received 8 January 2020; accepted 25 May 2020; published 8 June 2020)

Quasinormal modes of scalar field and electromagnetic field in a specific Finslerian-Schwarzschild spacetime have been investigated in this paper. The equations of motion for scalar field and electromagnetic field have been constructed by Finslerian-Laplace operator and divergence operator. The solutions of the equations of motion are presented. The solutions of angular part for scalar field and electromagnetic field are different. The solutions of radial part are numerically analyzed via WKB approximation and finite difference method, which give the quasinormal frequencies and dynamic evolution of quasinormal modes, respectively. The spectrum splitting generated from spherical symmetry breaking of the Finslerian-Schwarzschild spacetime is shown. The analysis of the dynamical evolution of quasinormal modes shows that the Finslerian-Schwarzschild black hole is stable if the Finslerian parameter $\epsilon^2 < 0.8$.

DOI: 10.1103/PhysRevD.101.124012

I. INTRODUCTION

The black hole, as one of the important predictions of general relativity, has been discussed intensively by physicists and tested by astronomical observations. Recent observations on gravitational waves have opened a new window to investigate the properties of black holes [1]. Currently, the first and second observing runs of Advanced LIGO detectors have identified ten gravitational wave events produced by the merge of binary black holes [2]. The ringdown phase, as one of the three processes of the merge of binary black holes, has deep connection with the quasinormal modes (QNMs). QNMs, described as the "characteristic sound" of black holes, have been studied to analyze the intrinsic properties of black holes [3–5] for a long time. The frequencies of QNMs, derived from the perturbed gravitational field equations on a black hole background, play an important role in determining the frequencies of gravitational waves in ringdown phase [3–5]. Ongoing third generation of gravitational wave detectors, such as Einstein Telescope [6], will provide more precise observations on the ringdown phase. However, space detectors, such as LISA [7] and Taiji [8], will give the observations on the ringdown phase in different frequency band. Recently, black hole detectability of LISA has been discussed [9] and Tso [10] studied to detect black hole spectroscopy by optimizing LIGO with LISA.

Though general relativity has been tested by various observations with high precisions [11], it is a classical theory and not compatible with standard quantum field theory. This fact is one of the major motivations that physicists constructed modified theories of gravity. Various modified theories of gravity have been tested by present astronomical observations [12]. The observations of gravitational waves open a window to test general relativity in strong gravity region. Different modified theories of gravity would give different modified gravitational field equations and generate different eigenfrequencies of QNMs. Thus, observations of the ringdown phase of gravitational waves provide an approach to test modified theories of gravity. In the framework of gauge-gravity duality, QNMs are reviewed in Refs. [13,14]. QNMs in extra dimensions are discussed in Refs. [15,16]. QNMs in higher-derivative gravity, such as $f(R)$ gravity and Horndeski gravity, are discussed in Refs. [17–19]. In the modified theories of gravity mentioned above, they share one common feature, namely, the background geometry which is Riemannian. And QNMs are derived from the Riemannian spacetime with spherical symmetry or axial symmetry.

Finsler geometry is a natural extension of Riemann geometry with latter as its special case [20]. Chern [20] has indicated that Finsler geometry is Riemannian geometry without the quadratic restriction. Generally, the Finslerian extension of a given Riemannian spacetime has less symmetry than the Riemannian spacetime [21,22]. By this basic feature of Finsler geometry, Finsler geometry is used to describe violation of Lorentz invariance [23–26] and study the anisotropy of our universe [27–29]. The constructions of the Finslerian gravitational field equation have been investigated in Refs. [30–35]. However, these equations are not equivalent to each other. At present, it is still an open debate that Finslerian generalizations of gravitational field equations are physically relevant. Thus, it is significant to

*lixin1981@cqu.edu.cn
†zhaosp@cqu.edu.cn

investigate physical predictions of these Finslerian gravitational field equations and constrain them by observations.

Starting from the Finslerian gravitational field equation given by Rutz [32], we have presented a class of Finslerian-Schwarzschild solutions [36] and Finslerian Reissner-Nordström solutions [37], and we have shown that the Finslerian spacetime possesses an event horizon. In this paper, we will investigate QNMs originated from the Finslerian-Schwarzschild solutions. The scalar and electromagnetic QNM spectrum will be derived. The Finslerian Schwarzschild black hole breaks the spherical symmetry. It is expected that the QNM spectrum of Finslerian-Schwarzschild black hole possesses a similar property with QNM spectrum of Kerr black hole in general relativity, namely, spherical symmetry breaking causes the spectrum splitting.

This paper is organized as follows. In Sec. II, we briefly introduce the Finslerian-Schwarzschild solutions and present the Finslerian-Laplace operator and divergence operator. Then, we derive the solutions of equations of motion of scalar field and electromagnetic field, respectively. In Sec. III, we utilize WKB approximation and finite difference method to analyze quasinormal frequencies and dynamic evolution of QNMs, respectively. Finally, discussions and conclusions are presented in Sec. IV.

II. QUASINORMAL MODES IN FINSLERIAN-SCHWARZSCHILD SPACETIME

A. Finslerian-Schwarzschild spacetime

Instead of defining an inner product structure over the tangent bundle in Riemann geometry, Finsler geometry is based on the so-called Finsler structure F with the property $F(x,\lambda y)=\lambda F(x,y)$ for all $\lambda>0$, where $x\in M$ represents position and $y\equiv\frac{dx}{d\tau}$ represents velocity. The Finslerian metric is given as [20]

$$g_{\mu\nu}\equiv\frac{\partial}{\partial y^\mu}\frac{\partial}{\partial y^\nu}\left(\frac{1}{2}F^2\right). \tag{1}$$

In Ref. [20], the Finsler structure is positive definite. However, in physics, the Finsler structure F is not positive definite at every point of the Finsler manifold. A positive, zero, or negative F corresponds to timelike, null, or spacelike curves, respectively. Recently, Javaloyes and Sanch [38] have presented a well-defined definition on the Finsler structure with Finsler metric of Lorentzian signature.

Rutz [32] has suggested that Finslerian vacuum gravitational field equation is vanishing from the Ricci scalar. The Ricci scalar is given as

$$Ric\equiv\frac{1}{F^2}\left(2\frac{\partial G^\mu}{\partial x^\mu}-y^\lambda\frac{\partial^2G^\mu}{\partial x^\lambda\partial y^\mu}+2G^\lambda\frac{\partial^2G^\mu}{\partial y^\lambda\partial y^\mu}-\frac{\partial G^\mu}{\partial y^\lambda}\frac{\partial G^\lambda}{\partial y^\mu}\right), \tag{2}$$

where

$$G^\mu=\frac{1}{4}g^{\mu\nu}\left(\frac{\partial^2F^2}{\partial x^\lambda\partial y^\nu}y^\lambda-\frac{\partial F^2}{\partial x^\nu}\right) \tag{3}$$

is called geodesic spray coefficients. In our previous research [36], we obtained the following Finslerian-Schwarzschild solution from the Finslerian vacuum gravitational field equation:

$$F^2=-\left(1-\frac{2GM}{r}\right)y^ty^t+\left(1-\frac{2GM}{r}\right)^{-1}y^ry^r+r^2\bar{F}^2, \tag{4}$$

where $\bar{F}$ is a two-dimensional Finsler space with positive constant flag curvature. Unlike Riemann geometry, Finsler spacetime with positive constant flag curvature is not equivalent to each other. For example, we obtained a Finsler spacetime with constant flag curvature [37], which admits four independent Killing vectors. In Ref. [22], we have shown that a projectively flat Randers spacetime with a constant flag curvature admits six independent Killing vectors, which implies these two Finsler spacetimes are not equivalent. As for two-dimensional Finsler space, Byrant [39] has given a projectively flat Finsler two-sphere of constant flag curvature. It is not equivalent to the Finsler space given by Shen [40]. Therefore, the Finslerian-Schwarzschild solution represents a class of black hole solutions in Finsler spacetime. Thus, physical observations, such as QNMs, could tell us which Finsler space with constant curvature is preferred.

In this paper, we only consider the Finslerian-Schwarzschild spacetime in which its subspace $\bar{F}$ takes the special form as follows [36,40]:

$$\bar{F}=\frac{\sqrt{(1-\epsilon^2\sin^2\theta)y^\theta y^\theta+\sin^2\theta y^\varphi y^\varphi}}{1-\epsilon^2\sin^2\theta}-\frac{\epsilon\sin^2\theta y^\varphi}{1-\epsilon^2\sin^2\theta}, \tag{5}$$

where ϵ is the Finslerian parameter and $0\leq\epsilon<1$. While $\epsilon=0$, the Finslerian-Schwarzschild spacetime reduces to Schwarzschild spacetime.

B. Scalar field perturbation of Finslerian-Schwarzschild black hole

In general relativity, most QNMs of Schwarzschild black hole can be unitarily described by the following wave function [14]:

$$\Psi=e^{-i\omega t}Y_l^m(\theta,\varphi)R(r). \tag{6}$$

The term $e^{-i\omega t}$ in formula (6) represents the temporal translation symmetry preserved in Schwarzschild spacetime. The spherical harmonics $Y_l^m(\theta,\varphi)$ in formula (6) represent the spherical symmetry preserved in Schwarzschild spacetime, which is derived from the Riemannian-Laplace operator. The term $R(r)$ satisfies the Schrödinger-like equation where its effective potential is of the form [14]

$$V^{GR} = f\left(\frac{l(l+1)}{r^2} + \frac{1}{r}\frac{df}{dr}(1-s^2)\right), \tag{7}$$

where s denotes spin of the investigated field. It is worth investigating whether the form of effective potential still holds or not in Finslerian-Schwarzschild spacetime.

In general relativity, the equations of motion of the scalar field and electromagnetic field relate to the Laplace operator and divergence operator, respectively. Thus, to find the equations of motion of the scalar field and electromagnetic field in Finslerian gravity, we should first investigate these operators in Finsler geometry. The Laplace operator in Riemannian geometry has good property that Laplace operators defined from several different ways [41] are equivalent to each other. However, Finslerian extension of these definitions will lead to different Laplace operators. Various Finslerian-Laplace operators are, respectively, defined by Bao and Lackey [42], Shen [43], Barthelme [44], and Mo [45]. In Ref. [46], another definition of Finslerian operator is given, namely, the mean Laplace operator. It proves that this Finslerian operator is equivalent to the one defined in Refs. [44,45]. The Finslerian-Laplace operator defined in Ref. [43] is not linear. Thus, it cannot be used to discuss QNMs. Since the Finslerian operator defined by Mo [45] is a linear operator and is equivalent to other two definitions [44,46], we consider Mo's definition [45] for convenience to discuss QNMs in this paper.

For any one form $A = A_\mu dx^\mu$ and smooth function ϕ, the Finslerian-Laplace operator and divergence operator [45] are given as

$$\Delta\phi = \sigma^{-1}\partial_\mu(\bar{g}^{\mu\nu}\sigma\partial_\nu\phi), \tag{8}$$

$$\mathrm{div}A = \sigma^{-1}\partial_\mu(\bar{g}^{\mu\nu}\sigma\partial A_\nu), \tag{9}$$

where σ denotes the Holmes-Thompson volume element in Finsler geometry [43]. $\bar{g}^{\mu\nu}$ is defined in terms of the Finsler metric $g^{\mu\nu}$,

$$\bar{g}^{\mu\nu} = \sigma^{-1}c_{n-1}^{-1}\int_{S_xM} g^{\mu\nu}\det(g_{\mu\nu}/F)d\eta, \tag{10}$$

where c_{n-1} denotes the volume of the unit Euclidean $(n-1)$ sphere, $S_xM = \{y \in T_xM | F(y) = 1\}$, and

$$d\eta = \sum_{i=1}^{n}(-1)^{i-1}y^i dy^1 \wedge \cdots \wedge \widehat{dy^i} \wedge \cdots \wedge dy^n. \tag{11}$$

However, the Holmes-Thompson volume element is given as

$$\sigma = c_{n-1}^{-1}\int_{S_xM}\det(g_{\mu\nu}/F)d\eta. \tag{12}$$

It should be noticed that $\bar{g}^{\mu\nu}$ is the Riemannian metric. Thus, the Finslerian-Laplace operator defined in Refs. [44–46] is a weighted Riemannian-Laplace operator. Though the Finslerian-Laplace operator and divergence operator are very similar to the Riemannian one, they still carry important information on Finsler spacetime, such as the Holmes-Thompson volume element σ. And the Riemannian metric $\bar{g}^{\mu\nu}$ can be regarded as an average one of Finsler metric $g^{\mu\nu}$.

In two-dimensional Randers space [47], i.e., $F = \sqrt{a_{ij}(x)y^i y^j} + b_i(x)y^i$, the mean Riemannian metric can be derived from the formula (10) [46]

$$\bar{g}_{ij} = \frac{1+\sqrt{1-b^2}}{2}a_{ij} - \frac{1}{2}b_i b_j, \tag{13}$$

where $b^2 \equiv a^{ij}b_i b_j$. The Holmes-Thompson volume element σ for Randers space is given as

$$\sigma = \sqrt{\det a_{ij}}. \tag{14}$$

Making use of the formulas (13) and (14), one can derive the Finslerian-Laplace operator for Randers space,

$$\Delta_{\bar{F}} = \frac{2(1-\epsilon^2\sin^2\theta)^{3/2}}{\sin^2\theta(1+\sqrt{1-\epsilon^2\sin^2\theta})}\frac{\partial^2}{\partial\varphi^2} + \frac{2(1-\epsilon^2\sin^2\theta)}{1+\sqrt{1-\epsilon^2\sin^2\theta}}\frac{\partial^2}{\partial\theta^2} + \frac{2\cos\theta(\epsilon^2\sin^2\theta+\sqrt{1-\epsilon^2\sin^2\theta})}{\sin\theta(1+\sqrt{1-\epsilon^2\sin^2\theta})}\frac{\partial}{\partial\theta}. \tag{15}$$

In this paper, we only consider the Finslerian effect for QNMs as a perturbation. Thus, we expand the Finslerian-Laplace operator $\Delta_{\bar{F}}$ in powers of ϵ. To first order in ϵ^2, the Finslerian-Laplace operator is given as

$$\Delta_{\bar{F}} = \frac{1}{\sin\theta}\left(1-\frac{3}{2}\epsilon^2\sin^2\theta\right)\left(\partial_\theta\sin\theta\left(1+\frac{3}{4}\epsilon^2\sin^2\theta\right)\partial_\theta\right) + \frac{1}{\sin^2\theta}\left(1-\frac{5}{4}\epsilon^2\sin^2\theta\right)\partial_\varphi^2. \tag{16}$$

From the definition of mean Riemannian metric, one can find that $\bar{g}^{\mu\nu} = g^{\mu\nu}$ if $g^{\mu\nu}$ is Riemannian metric. The Finslerian-Schwarzschild metric is a warp product metric. And nonquadratic components of the Finslerian-Schwarzschild metric only appear in angular part of this spacetime. Thus, the Finslerian-Laplace operator for the Finslerian-Schwarzschild spacetime has the form

$$\Delta_F = -f^{-1}\partial_t^2 + r^{-2}\partial_r(fr^2\partial_r) + \Delta_{\bar{F}}, \tag{17}$$

where $f \equiv 1\text{–}2GM/r$. Then, the equation of motion of the massless scalar field Ψ in Finslerian-Schwarzschild spacetime satisfies

$$\Delta_F \Psi = 0. \tag{18}$$

The solution of Eq. (18) is given as

$$\Psi = e^{-i\omega t} \bar{Y}_l^m(\theta, \varphi) R^S(r)/r. \tag{19}$$

The $\bar{Y}_l^m(\theta, \varphi)$ in Eq. (19) is the eigenfunction of the Finslerian-Laplace operator $\Delta_{\bar{F}}$,

$$\bar{Y}_l^m = Y_l^m + \epsilon^2 (\bar{C}_{l+2}^m Y_{l+2}^m + \bar{C}_{l-2}^m Y_{l-2}^m), \tag{20}$$

where

$$\bar{C}_{l+2}^m = -\frac{3l(l-1)}{8(2l+3)^2} \times \sqrt{\frac{(l+m+1)(l-m+1)(l+m+2)(l-m+2)}{(2l+1)(2l+5)}}, \tag{21}$$

$$\bar{C}_{l-2}^m = \frac{3(l+1)(l+2)}{8(2l-1)^2} \sqrt{\frac{(l+m)(l-m)(l+m-1)(l-m-1)}{(2l+1)(2l-3)}}. \tag{22}$$

Moreover, the corresponding eigenvalue of the Finslerian-Laplace operator $\Delta_{\bar{F}}$ is given as [37]

$$\lambda^S = l(l+1) + \lambda_M^S, \tag{23}$$

where $\lambda_M^S = -\epsilon^2 (\frac{3(l-1)l(l+1)(l+2)}{2(2l-1)(2l+3)} + \frac{m^2(7l^2+7l+6)}{2(2l-1)(2l+3)})$ is the modified eigenvalue of scalar field perturbations derived from the Finslerian-Schwarzschild spacetime.

The $R^S(r)$ in Eq. (18) satisfies the following Schrödinger-like equation:

$$\frac{d^2 R^S}{dr_*^2} + (\omega^2 - V^S) R^S = 0, \tag{24}$$

where $dr_* = dr/f$ is the tortoise coordinate, and the effective scalar potential is given as

$$V^S = f\left(\frac{\lambda^S}{r^2} + \frac{1}{r}\frac{df}{dr}\right). \tag{25}$$

The difference between the Finslerian-Schwarzschild spacetime and Schwarzschild spacetime lies on angular components of spacetime metric. It also reflects on the solution of equation of motion of massless scalar field. However, in standard process of dealing with QNMs, only the nonangular solution is physically important, i.e., $e^{-i\omega t} R^S(r)/r$. The Schrödinger-like equation will give a wavelike solution. And it possesses a complex frequency generated from the effective scalar potential V^S. This is the reason why physicists call such phenomena QNMs. The effective scalar potential V^S implies the Finslerian effect on QNMs comes from the eigenvalue λ^S of the Finslerian-Laplace operator $\Delta_{\bar{F}}$, which depends on multipole quantum number l, magnetic quantum number m, and the Finslerian parameter ϵ.

C. Electromagnetic field perturbation of Finslerian-Schwarzschild black hole

The electromagnetic field on Finslerian spherical bundle has been studied in Ref. [48]. Unlike the researches in Ref. [48], we investigate electromagnetic field in terms of the mean Riemannian metric $\bar{g}_{\mu\nu}$. Following the same reason of constructing the Finslerian-Laplace operator for the Finslerian-Schwarzschild spacetime, the equation of motion of electromagnetic field can be constructed by the Finslerian divergence operator. It is of the form

$$\frac{1}{\sqrt{-g}} (\partial_\nu \sqrt{-g} F^{\nu\mu}) = 0, \tag{26}$$

where $g = r^2 \sigma$ denotes the determinant of the mean Riemannian metric $\bar{g}_{\mu\nu}$ of Finslerian-Schwarzschild spacetime, and $F^{\nu\mu} = \bar{g}^{\nu\alpha} \bar{g}^{\mu\beta} F_{\alpha\beta}$. The electromagnetic tensor $F_{\mu\nu}$ is given via vector potential A^μ,

$$F_{\mu\nu} = \partial_\mu A_\nu - \partial_\nu A_\mu. \tag{27}$$

In Schwarzschild spacetime, the equation of motion of electromagnetic field can be solved by Ruffni's approach [49], namely, expanding vector potential A_μ in vector spherical harmonics. However, the spherical symmetry does not hold in Finslerian-Schwarzschild spacetime. It is difficult to find an exact solution of Eq. (26). In this paper, we find a perturbed solution of Eq. (26). The vector potential A_μ is an extension of the axial mode of Ruffini's solution [49]. The nonvanishing components of A_μ are of the form

$$A_\theta = e^{-i\omega t} R^A(r) \frac{1}{\sin\theta} \left(1 - \frac{3}{4}\epsilon^2 \sin^2\theta\right) \partial_\varphi \tilde{Y}_l^m(\theta, \varphi), \tag{28}$$

$$A_\varphi = -e^{-i\omega t} R^A(r) \sin\theta \left(1 - \frac{1}{4}\epsilon^2 \sin^2\theta\right) \partial_\theta \tilde{Y}_l^m(\theta, \varphi). \tag{29}$$

By making use of the Finslerian-Schwarzschild metric, and substituting the formulas of vector potential A_μ into Eq. (26), to first order in ϵ^2, one can find that Eq. (26) can be simplified into the following equations:

$$\frac{d^2R^A}{dr_*^2} + (\omega^2 - V^A)R^A = 0, \tag{30}$$

$$\Delta^A_{\bar{F}}\tilde{Y}^m_l(\theta,\varphi) + \lambda^A\tilde{Y}^m_l(\theta,\varphi) = 0, \tag{31}$$

where the effective potential of axial mode of electromagnetic field V^A is given as

$$V^A = \frac{f\lambda^A}{r^2}, \tag{32}$$

and the operator $\Delta^A_{\bar{F}}$ is defined as

$$\Delta^A_{\bar{F}} \equiv \frac{1}{\sin\theta}\left(1-\frac{1}{2}\epsilon^2\sin^2\theta\right)\left(\partial_\theta\sin\theta\left(1-\frac{1}{4}\epsilon^2\sin^2\theta\right)\partial_\theta\right) + \frac{1}{\sin^2\theta}\left(1-\frac{5}{4}\epsilon^2\sin^2\theta\right)\partial^2_\varphi. \tag{33}$$

The $\tilde{Y}^m_l(\theta,\varphi)$ in Eqs. (28) and (29) is the eigenfunction of the operator $\Delta^A_{\bar{F}}$,

$$\tilde{Y}^m_l = Y^m_l + \epsilon^2(\tilde{C}^m_{l+2}Y^m_{l+2} + \tilde{C}^m_{l-2}Y^m_{l-2}), \tag{34}$$

where

$$\tilde{C}^m_{l+2} = -\frac{l(3l+5)}{8(2l+3)^2} \times\sqrt{\frac{(l+m+1)(l-m+1)(l+m+2)(l-m+2)}{(2l+1)(2l+5)}}, \tag{35}$$

$$\tilde{C}^m_{l-2} = \frac{(3l-2)(l+1)}{8(2l-1)^2}\sqrt{\frac{(l+m)(l-m)(l+m-1)(l-m-1)}{(2l+1)(2l-3)}}. \tag{36}$$

Moreover, the corresponding eigenvalue of the operator $\Delta^A_{\bar{F}}$ is given as

$$\lambda^A = l(l+1) + \lambda^A_M, \tag{37}$$

where $\lambda^A_M = -\epsilon^2\left(\frac{l(l+1)(3l^2+3l-2)}{2(2l-1)(2l+3)} + \frac{m^2(7l^2+7l-6)}{2(2l-1)(2l+3)}\right)$ is the modified eigenvalue of electromagnetic field perturbations derived from the Finslerian-Schwarzschild spacetime.

One should notice that the operator $\Delta^A_{\bar{F}}$ differs from the Finslerian-Laplace operator $\Delta_{\bar{F}}$. It means that the solutions of angular part for scalar field and electromagnetic field are different. This is another feature of QNMs in Finslerian-Schwarzschild spacetime.

In the above discussion, we have presented the extension of the axial mode of Ruffini's solution [49]. Now, we will give an extension of the polar mode of Ruffini's solution. The nonvanishing components of $\bar{A}_\mu$ for the polar mode extension are of the form

$$\bar{A}^T_\mu = \left[a_1(r,t)\bar{Y}^m_l, a_2(r,t)\bar{Y}^m_l, a_3(r,t)\frac{\partial\bar{Y}^m_l}{\partial\theta}, a_3(r,t)\frac{\partial\bar{Y}^m_l}{\partial\varphi}\right], \tag{38}$$

where $\bar{Y}^m_l$ is the same with the one in scalar perturbation and satisfies the equation (20). Following the method proposed in Ref. [49], a master variable is defined as

$$R^P(r) \equiv e^{i\omega t}\frac{r^2}{\lambda^S}\left(\frac{\partial a_2}{\partial t} - \frac{\partial a_1}{\partial r}\right). \tag{39}$$

By making use of the Finslerian-Schwarzschild metric, and substituting the formulas of vector potential $\bar{A}_\mu$ into Eq. (26), to first order in ϵ^2, one can find that the master variable R^P satisfies the following equation:

$$\frac{d^2R^P}{dr_*^2} + (\omega^2 - V^P)R^P = 0, \tag{40}$$

where the effective potential of polar mode of electromagnetic field V^P is given as

$$V^P = \frac{f\lambda^S}{r^2}. \tag{41}$$

III. NUMERICAL RESULTS

A. Dependence of parameters from WKB approximation

In Sec. II, we found that both the scalar field and electromagnetic field satisfy the Schrödinger-like equations (24), (30), and (40), respectively. Therefore, the characteristic frequency of the corresponding QNMs can be obtained from the WKB approximation. Such method was proposed by Schutz and Will [50] and then promoted by Iyer and Will [51] and Konoplya [52]. Here, we use sixth order WKB approximation [52] with high accuracy, which has the form

$$\left.\frac{i(\omega^2 - V_0)}{\sqrt{-2V''_0}}\right|_{r=r_0} = n + \frac{1}{2} + \sum_{i=2}^{6}\Lambda_i, \quad (n = 0,1,2,\ldots), \tag{42}$$

where V_0 is the maximum value of effective potential, Λ_i is the ith order correction terms depending on the effective potential, and the specific forms of the corrections can be found in Refs. [50–52]. In this paper, we mainly consider the fundamental QNMs frequencies which are described by overtone number $n = 0$.

WKB approximation is directly related to the effective potential. In Finslerian-Schwarzschild black hole, the

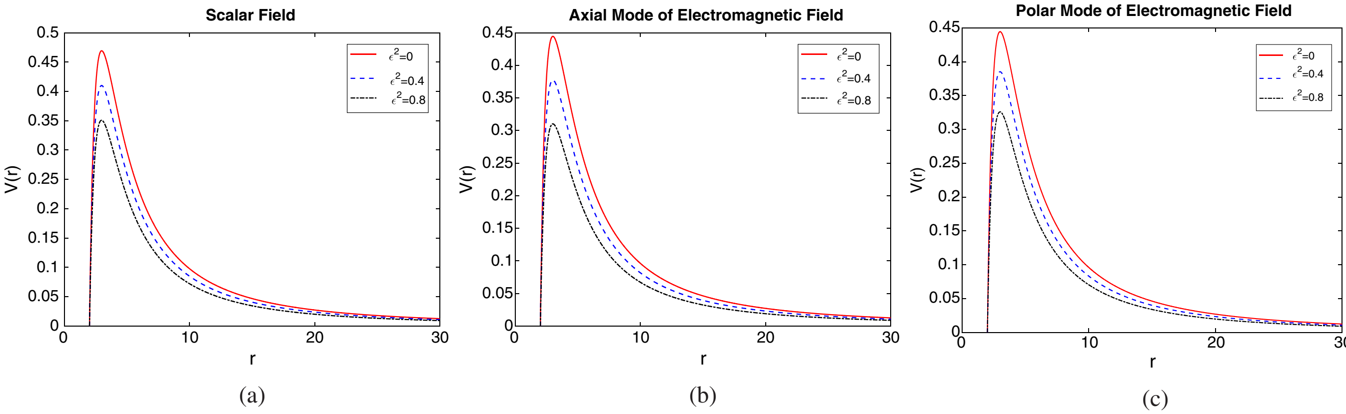

FIG. 1. The effective scalar potential, axial and polar modes of electromagnetic potential in Finslerian-Schwarzschild spacetime with different ϵ^2. The parameters used in the calculation were $GM = 1$, $m = 0$, $l = 3$.

effective scalar potential and electromagnetic potential are given by Eqs. (25), (32), and (41), as illustrated in Fig. 1. It is obvious that the effective electromagnetic potential is smaller than scalar potential under the same parameters. Both the effective potentials of scalar field and electromagnetic field vanish while r approaches to event horizon of Finslerian-Schwarzschild black hole and infinity. Following the discussion in the review paper [13], one can find that our Schrödinger-like equations should possess the same boundary condition with the one in Schwarzschild spacetime. Thus, the Schrödinger-like equations satisfy the following ingoing and outgoing boundary conditions:

$$\lim_{r_* \to \mp\infty} \pm R \exp(\pm i\omega r_*) = 1. \tag{43}$$

The complex frequencies of QNMs in Finslerian-Schwarzschild spacetime are related to the effective potential that depends on four parameters, i.e., the mass of black hole GM, Finslerian parameter ϵ^2, and multipole quantum number l and magnetic quantum number m. In this paper, we just analyze dimensionless quasinormal frequencies. The mass of black hole has been set as $GM = 1$ in the following numerical calculations. The Finslerian parameter ϵ^2 is an essential quantity that measures the deviation from Schwarzschild spacetime to Finslerian spacetime. Thus, we

TABLE I. Fundamental quasinormal frequencies for scalar field and axial and polar modes of electromagnetic field perturbations with various values of l and ϵ^2. It is calculated by sixth order WKB approximation and the parameters used in the calculation were $GM = 1$ and $m = 0$.

				Electromagnetic			
		Scalar		Axial		Polar	
l	ϵ^2	Re(ω_0)	Im(ω_0)	Re(ω_0)	Im(ω_0)	Re(ω_0)	Im(ω_0)
0	0.1	0.110460	−0.1008230	…	…	…	…
1	0.1	0.292910	−0.0977616	0.242191	−0.0924927	0.248191	−0.0926370
	0.2	0.292910	−0.0977616	0.236041	−0.0923365	0.248191	−0.0926370
	0.3	0.292910	−0.0977616	0.229731	−0.0921671	0.248191	−0.0926370
	0.4	0.292910	−0.0977616	0.223247	−0.0919826	0.248191	−0.0926370
	0.5	0.292910	−0.0977616	0.216574	−0.0917810	0.248191	−0.0926370
2	0.1	0.477033	−0.0967815	0.448256	−0.0949633	0.450609	−0.0949756
	0.2	0.470332	−0.0967978	0.438721	−0.0949115	0.443514	−0.0949379
	0.3	0.463534	−0.0968151	0.428975	−0.0948553	0.436305	−0.0948979
	0.4	0.456635	−0.0968335	0.419003	−0.0947940	0.428975	−0.0948553
	0.5	0.449630	−0.0968531	0.408789	−0.0947271	0.421518	−0.0948099
3	0.1	0.664308	−0.0965099	0.643995	−0.0955933	0.645526	−0.0955962
	0.2	0.653062	−0.0965198	0.630828	−0.0955675	0.633950	−0.0955737
	0.3	0.641620	−0.0965305	0.617380	−0.0955395	0.622159	−0.0955497
	0.4	0.629970	−0.0965420	0.603633	−0.0955091	0.610141	−0.0955237
	0.5	0.618100	−0.0965543	0.589566	−0.0954758	0.597881	−0.0954957

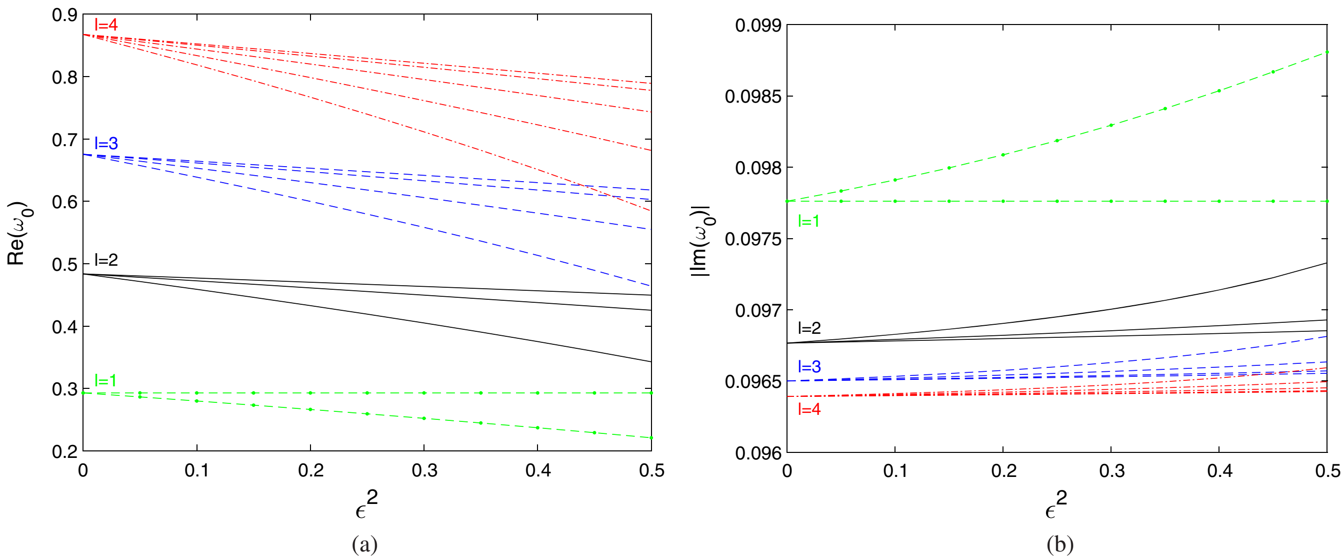

FIG. 2. Real and imaginary part of fundamental quasinormal frequencies of scalar field perturbations with $l = 1, 2, 3, 4$ and varying m. Lines refer to $m = 0, \ldots, l$ from top to bottom for $\mathrm{Re}(\omega_0)$, and from bottom to top for $|\mathrm{Im}(\omega_0)|$.

first analyze the dependence of fundamental quasinormal frequencies with ϵ^2. The numerical results are listed in Table I. For scalar field, the magnitude of $\mathrm{Re}(\omega_0)$ decreases as ϵ^2 increases, the magnitude of $|\mathrm{Im}(\omega_0)|$ increases as ϵ^2 increase. For axial mode of electromagnetic field and polar mode of electromagnetic field with $l > 1$, the magnitudes of $\mathrm{Re}(\omega_0)$ and $|\mathrm{Im}(\omega_0)|$ are both suppressed with higher ϵ^2. The different behaviors of the magnitude of $|\mathrm{Im}(\omega_0)|$ between scalar field and electromagnetic field just reflect the difference between the eigenvalues of operator $\Delta_{\bar{F}}$ and $\Delta^A_{\bar{F}}$. It should be noticed that, in Table I, the fundamental QNM frequencies of scaler field perturbations and polar mode of electromagnetic field perturbations in Finslerian-Schwarzschild spacetime are the same with the one in Schwarzschild spacetime if $l = 0, 1$ and $m = 0$, which just reflects that the eigenvalue $\lambda^S = \lambda_{GR}$ if $l = 0, 1$ and $m = 0$.

Similar to the Kerr QNM spectrum, spherical symmetry breaking causes Zeeman-like splitting of QNM spectrum in Finslerian-Schwarzschild spacetime. The impacts of m on the fundamental quasinormal frequencies are shown in Figs. 2–4. The numerical results calculated by the WKB approximation are reported in Table II. For scalar field, the magnitude of $\mathrm{Re}(\omega_0)$ decreases with higher m, and the magnitude of $|\mathrm{Im}(\omega_0)|$ increases as m increases.

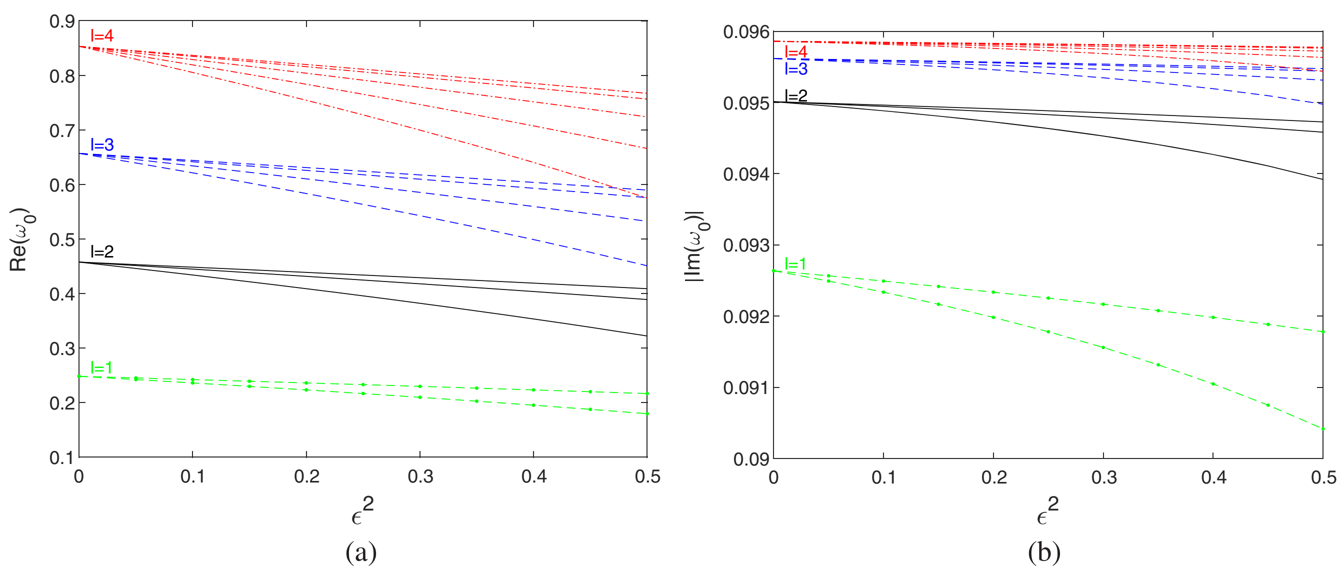

FIG. 3. Real and imaginary part of fundamental quasinormal frequencies of axial mode of electromagnetic field perturbations with $l = 1, 2, 3, 4$ and varying m. Lines refer to $m = 0, \ldots, l$ from top to bottom for $\mathrm{Re}(\omega_0)$ and $|\mathrm{Im}(\omega_0)|$.

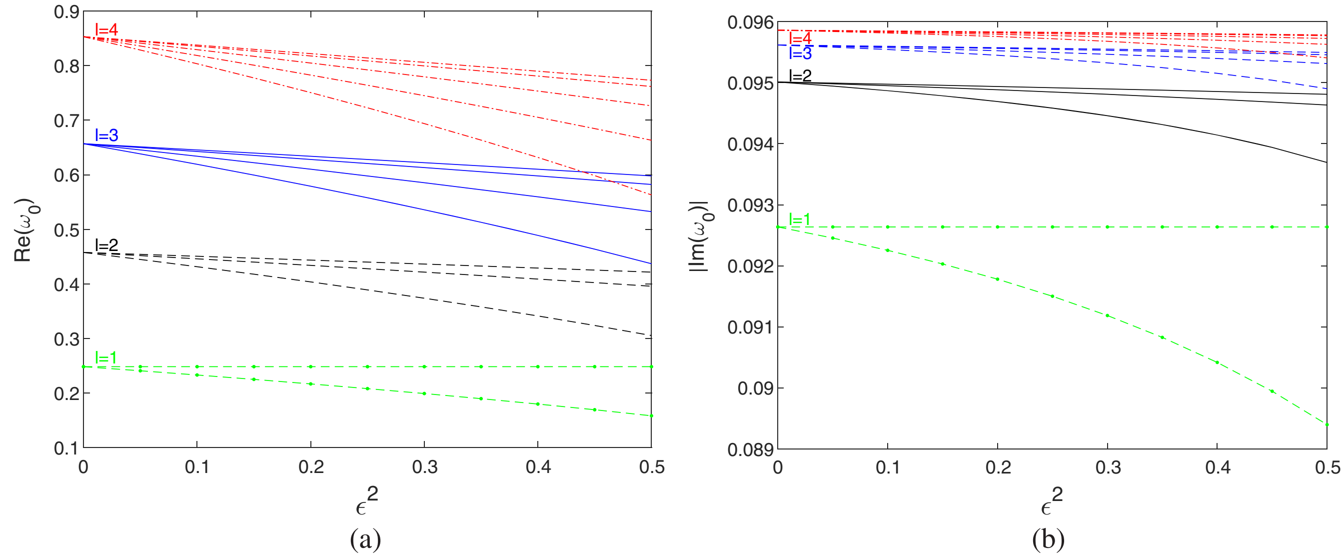

FIG. 4. Real and imaginary part of fundamental quasinormal frequencies of polar mode of electromagnetic field perturbations with $l = 1, 2, 3, 4$ and varying m. Lines refer to $m = 0, \ldots, l$ from top to bottom for $\mathrm{Re}(\omega_0)$ and $|\mathrm{Im}(\omega_0)|$.

For axial and polar modes of electromagnetic field, the magnitudes of $\mathrm{Re}(\omega_0)$ and $|\mathrm{Im}(\omega_0)|$ both decrease with higher m.

B. Stability analysis from finite difference method

The four-dimensional Schwarzschild black hole is stable under perturbations [53]. The stability of black hole guarantees its theoretical existence in cosmology. Thus, it is important to test the stability of Finslerian-Schwarzschild black hole. The stability is controlled by the effective potential. The black hole is stable if the effective potential is positive definite. While the eigenvalues $\lambda^S > 0$ and $\lambda^A > 0$, then the effective potentials of scalar field and electromagnetic field are positive definite, respectively. Both the eigenvalues λ^S and λ^A have the same lower bound if $m = l$ and $l \to \infty$, and it is of the form

$$\lim_{l\to\infty} \lambda^S = \lim_{l\to\infty} \lambda^A = l^2(1 - 5\epsilon^2/4). \tag{44}$$

The formula (44) implies that the Finslerian-Schwarzschild black hole is stable if $\epsilon^2 < 0.8$. One should notice that our analysis for stability is derived from a perturbative approach. We will test this stability analysis via the dynamical evolution of QNMs.

Finite difference method [54], extensively used with discretization and Taylor expansion, has been adopted to analyze the dynamical evolution of QNMs. Introducing the light-cone coordinates $\mu = t - r_*$ and $\nu = t + r_*$, the wave equations (24), (30) and (40) can be simplified into the following differential equation:

TABLE II. Fundamental quasinormal frequencies for scalar field and axial and polar modes of electromagnetic field perturbations with various values of l and m, calculated with the sixth order WKB approximation. For the considered spacetime, the parameters used in the calculation were $GM = 1$ and $\epsilon^2 = 0.5$.

				Electromagnetic			
		Scalar		Axial		Polar	
l	m	$\mathrm{Re}(\omega_0)$	$\mathrm{Im}(\omega_0)$	$\mathrm{Re}(\omega_0)$	$\mathrm{Im}(\omega_0)$	$\mathrm{Re}(\omega_0)$	$\mathrm{Im}(\omega_0)$
0	0	0.110460	−0.1008230	…	…	…	…
1	0	0.292910	−0.0977616	0.216574	−0.0917810	0.248191	−0.0926370
	1	0.221047	−0.0988080	0.179657	−0.0904171	0.158145	−0.0893976
2	0	0.449630	−0.0968531	0.408789	−0.0947271	0.421518	−0.0948099
	1	0.425448	−0.0969288	0.388919	−0.0945831	0.395653	−0.0946341
	2	0.342822	−0.0973295	0.322087	−0.0939193	0.305274	−0.0936923
3	0	0.618100	−0.0965543	0.589566	−0.0954758	0.597881	−0.0954957
	1	0.602935	−0.0965712	0.575799	−0.0954409	0.582194	−0.0954574
	2	0.554957	−0.0966343	0.532369	−0.0953138	0.532369	−0.0953138
	3	0.464104	−0.0968136	0.450804	−0.0949766	0.436910	−0.0949013

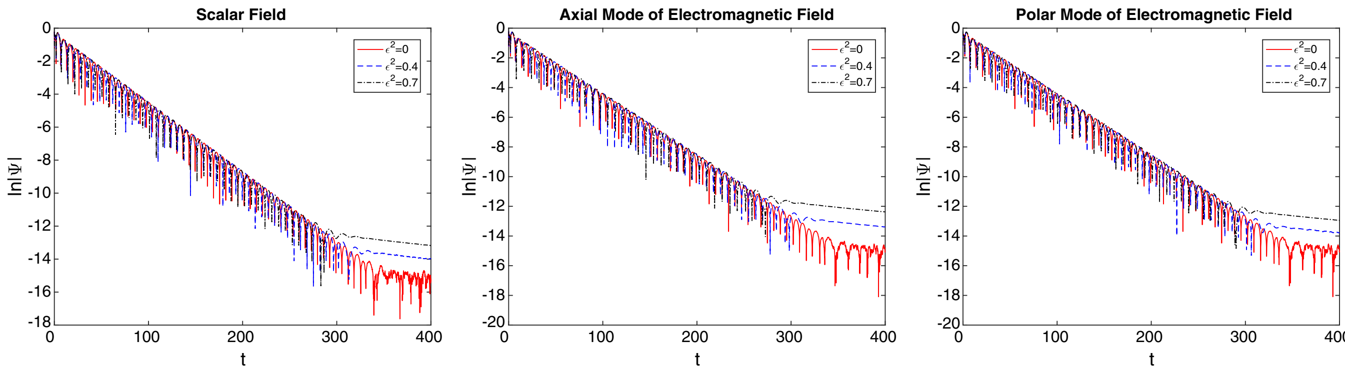

(a) (b) (c)

FIG. 5. The dynamical evolution of fundamental quasinormal of scalar field and axial and polar modes of electromagnetic field in Finslerian-Schwarzschild spacetime with different ϵ^2. The parameters used in the calculation were $GM = 1$, $l = 2$, $m = 0$.

$$\left(4\frac{\partial^2}{\partial\mu\partial\nu} + V(\mu,\nu)\right)\psi(\mu,\nu) = 0. \tag{45}$$

Using Taylor expansion, Eq. (45) can be discretized as

$$\begin{aligned}\psi(\mu+\delta\mu,\nu+\delta\nu) &= \psi(\mu,\nu+\delta\nu) + \psi(\mu+\delta\mu,\nu) - \psi(\mu,\nu)\\ &\quad - \Delta\mu\Delta\nu V\left(\frac{2\nu-2\mu+\delta\nu-\delta\mu}{4}\right)\frac{\psi(\mu+\delta\mu,\nu)+\psi(\mu,\nu+\delta\nu)}{8} + \mathcal{O}(h^4),\end{aligned} \tag{46}$$

where $h = \delta\mu = \delta\nu$ is the grid cell scale. We set $\psi(\mu,\nu = \nu_0) = 0$ as a boundary condition in the process of arithmetic, and the other one is a Gaussian pulse as the initial condition $\psi(\mu = \mu_0,\nu) = \exp[-(\nu-\nu_c)^2/2\omega^2]$. The constants of Gaussian pulse are fixed in following calculations, namely, $\nu_c = 1$ and $\omega = 1$.

The dynamical evolution of QNMs in Finslerian-Schwarzschild spacetime can be affected by multipole quantum number l, magnetic quantum number m, and the Finslerian parameter ϵ^2. The effects of these various parameters on the dynamical evolutions of scalar field and electromagnetic field are shown in Figs. 5–7, respectively. Our numerical results of the dynamical evolution of QNMs show that no instability occurs if $\epsilon^2 < 0.8$. It is consistent with the analysis of the effective potentials.

In the given figures, one can find that the periods of oscillation of scalar field and electromagnetic field both increase with higher Finslerian parameter ϵ^2 and higher magnetic quantum number m. And they both decrease with higher multipole quantum number l. One should notice that

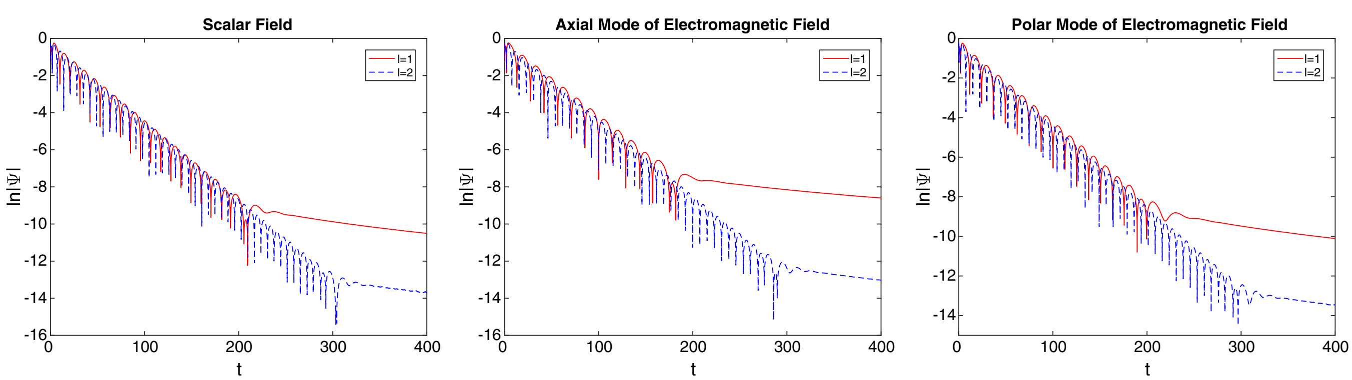

(a) (b) (c)

FIG. 6. The dynamical evolution of fundamental quasinormal of scalar field and axial and polar modes of electromagnetic field in Finslerian-Schwarzschild spacetime with different l. The parameters used in the calculation were $GM = 1$, $m = 0$, and $\epsilon^2 = 0.5$.

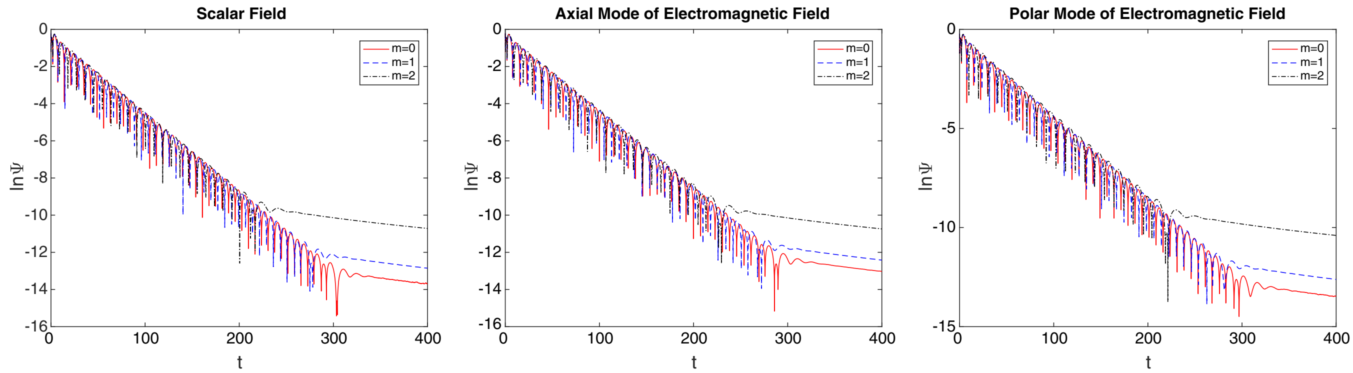

(a) (b) (c)

FIG. 7. The dynamical evolution of fundamental quasinormal of scalar field and axial and polar modes of electromagnetic field in Finslerian-Schwarzschild spacetime with different m. And m is a degenerate quantity in Finsler geometry. The parameters used in the calculation were $GM = 1$, $l = 2$, and $\epsilon^2 = 0.5$.

the periods of oscillation are proportional to the inverse of the real part of the QNMs frequencies. In the above figures on the dynamical evolution of QNMs, magnitude of the peak of the dynamical evolution of QNMs decreases with the increase in time. It denotes the effect of the imaginary part of the QNMs frequencies. The dependence between the parameters (ϵ^2, l, m) and the descent speed of the peak are not obvious in the above figures. Our numerical results of the dynamical evolution show that such dependence is the same with the numerical results obtained by the WKB approximation. Therefore, the results of dynamical evolutions of QNMs are compatible with the numerical results of WKB approximations that are presented in Sec. III A.

IV. DISCUSSIONS AND CONCLUSIONS

In this paper, we investigated QNMs of a specific Finslerian-Schwarzschild black hole. We adopted the Finslerian-Laplace operator and divergence operator defined in Ref. [45] to derive the equations of motion of scalar field and electromagnetic field. The solutions for scalar field and electromagnetic field are presented in Eqs. (19), (28), (29), and (38), respectively. The solutions of angular part for scalar field $\bar{Y}_l^m$ and electromagnetic field $\tilde{Y}_l^m$ are different, although both of them reduce to spherical harmonic function if the Finslerian parameter $\epsilon = 0$. We found that both solutions of the radial part for scalar field R^S and electromagnetic field R^A and R^P satisfy the Schrödinger-like equations, respectively. The difference between the eigenvalues λ^S and λ^A means that the Schrödinger-like equations cannot be written into a compact form as the one for Schwarzschild black hole.

The Schrödinger-like equations were solved via WKB approximation and finite difference method. Fundamental quasinormal frequencies for scalar field and electromagnetic field with various l and ϵ^2 are presented in Table I. The Finslerian parameter ϵ^2 does affect the period of oscillation of QNMs in Finslerian-Schwarzschild black hole. And it has less effect on the decay rate of QNMs. The effective potentials of scalar field and electromagnetic field depend on the magnetic quantum number m. Such a fact reflects the spherical symmetry breaking of Finslerian-Schwarzschild spacetime, and hence it will cause spectrum splitting. The results are listed in Table II. The difference between the eigenvalues λ^S and λ^A has impacted the spectrum splitting, shown in Figs. 2–4. One should notice that the spectrum splitting of QNMs in Finslerian-Schwarzschild black hole differs from the one in Kerr black hole. This is due to the fact that the effective potentials of scalar field and electromagnetic field depend on m^2 in Finslerian-Schwarzschild black hole and the one depends on m in Kerr black hole.

Both theoretical analysis on the effective potential and numerical calculations of the dynamical evolution of QNMs show that the Finslerian-Schwarzschild black hole is stable if the Finslerian parameter $\epsilon^2 < 0.8$. One should notice that our analysis for stability is derived from a perturbative approach. In all, our results show that the Finslerian-Schwarzschild black hole could exist in cosmology and its QNMs of scalar field and electromagnetic field possess distinguish properties from the one in Schwarzschild black hole or Kerr black hole.

At last, we should emphasize that QNMs obtained in this paper are based on the Finslerian gravitational field equation that was presented by Rutz [32]. Other Finslerian gravitational field equations [31,33,34] will derive different vacuum solutions. All of them are expected to be different from the Finslerian-Schwarzschild spacetime [36], since these gravitational field equations are not equivalent to each other. QNMs generated from these different vacuum solutions should be different. Therefore, the observations of QNMs will be an approach to distinguish which Finslerian gravitational field equations or Einstein's field equation is valid.

ACKNOWLEDGMENTS

We would like to thank Professor K. Lin and Professor J. Li for useful discussions. This work has been supported by the National Natural Science Fund of China (Grants No. 11775038 and No. 11947406).

[1] B. P. Abbott *et al.* (LIGO Scientific and Virgo Collaborations), Phys. Rev. Lett. **116**, 061102 (2016).
[2] B. P. Abbott *et al.* (LIGO Scientific and Virgo Collaborations), Phys. Rev. X **9**, 031040 (2019).
[3] H. P. Nollert, Classical Quantum Gravity **16**, R159 (1999).
[4] K. D. Kokkotas and B. G. Schmidt, Living Rev. Relativity **2**, 2 (1999).
[5] V. Ferrari and L. Gualtieri, Gen. Relativ. Gravity **40**, 945 (2008).
[6] B. Sathyaprakash *et al.*, Classical Quantum Gravity **29**, 124013 (2012).
[7] P. Amaro-Seoane *et al.*, arXiv:1702.00786.
[8] W. H. Ruan, Z. K. Guo, R. G. Cai, and Y. Z. Zhang, arXiv:1909.07104.
[9] M. L. Katz and S. L. Larson, Mon. Not. R. Astron. Soc. **483**, 3108 (2019).
[10] R. Tso, D. Gerosa, and Y.-B. Chen, Phys. Rev. D **99**, 124043 (2019).
[11] C. M. Will, Living Rev. Relativity **17**, 4 (2014); **4**, 4 (2001).
[12] E. Berti *et al.*, Classical Quantum Gravity **32**, 243001 (2015).
[13] E. Berti, V. Cardoso, and A. O. Starinets, Classical Quantum Gravity **26**, 163001 (2009).
[14] R. A. Konoplya and A. Zhidenko, Rev. Mod. Phys. **83**, 793 (2011).
[15] S. Chakraborty, K. Chakravarti, S. Bose, and S. SenGupta, Phys. Rev. D **97**, 104053 (2018).
[16] C. Molina, A. B. Pavan, and T. E. M. Torrejon, Phys. Rev. D **93**, 124068 (2016).
[17] J. L. Blazquez-Salcedo, D. D. Doneva, J. Kunz, K. V. Staykov, and S. S. Yazadjiev, Phys. Rev. D **98**, 104047 (2018).
[18] O. J. Tattersall and P. G. Ferreira, Phys. Rev. D **97**, 104047 (2018).
[19] S. Datta and S. Bose, Eur. Phys. J. C **80**, 14 (2020).
[20] D. Bao, S. S. Chern, and Z. Shen, *An Introduction to Riemann-Finsler Geometry* (Springer Press, New York, 2000), pp. 1–96.
[21] H. C. Wang, J. Math. Soc. **S1–22**, 5 (1947).
[22] X. Li and Z. Chang, Differential Geometry and its Applications **30**, 737 (2012).
[23] F. Girelli, S. Liberati, and L. Sindoni, Phys. Rev. D **75**, 064015 (2007).
[24] G. W. Gibbons, J. Gomis, and C. N. Pope, Phys. Rev. D **76**, 081701(R) (2007).
[25] Z. Chang and X. Li, Phys. Lett. B **663**, 103 (2008).
[26] V. A. Kostelecky, Phys. Lett. B **701**, 137 (2011); V. A. Kostelecky, N. Russell, and R. Tsoc, Phys. Lett. B **716**, 470 (2012).
[27] A. P. Kouretsis, M. Stathakopoulos, and P. C. Stavrinos, Phys. Rev. D **79**, 104011 (2009); **82**, 064035 (2010).
[28] X. Li, H.-N. Lin, S. Wang, and Z. Chang, Eur. Phys. J. C **75**, 181 (2015).
[29] X. Li, S. Wang, and Z. Chang, Eur. Phys. J. C **75**, 260 (2015); X. Li and S. Wang, Eur. Phys. J. C **76**, 51 (2016); X. Li and H.-N. Lin, Eur. Phys. J. C **77**, 316 (2017).
[30] X. Li and Z. Chang, Chin. Phys. C **34**, 28 (2010).
[31] R. Miron and M. Anastasiei, *The Geometry of Lagrange Spaces: Theory and Applications* (Kluwer Academic, Dordrecht, 1994).
[32] S. F. Rutz, Gen. Relativ. Gravit. **25**, 1139 (1993).
[33] S. Vacaru, P. Stavrinos, E. Gaburov, and D. Gonta, arXiv:gr-qc/0508023.
[34] C. Pfeifer and M. N. R. Wohlfarth, Phys. Rev. D **85**, 064009 (2012).
[35] P. Ni and B. Shen, Ann. Phys. (Amsterdam) **404**, 93 (2019).
[36] X. Li and Z. Chang, Phys. Rev. D **90**, 064049 (2014).
[37] X. Li, Phys. Rev. D **98**, 084030 (2018).
[38] M. A. Javaloyes and M. Sanch, arXiv:1805.06978.
[39] R. L. Bryant, Sel. Math. New Ser. **3**, 161 (1997).
[40] Z. Shen, Manuscr. Math. **109**, 349 (2002).
[41] S. Gallot, D. Hulin, and J. Lafontaine, *Riemannian Geometry*, 3rd ed., Universitext (Springer-Verlag, Berlin, 2004).
[42] D. Bao and B. Lackey, C. R. Acad. Sci. Paris **223**, 51 (1996).
[43] Z. Shen, *Lectures on Finsler Geometry* (World Scientific, Singapore, 2001).
[44] T. Barthelme, Isr. J. Math. **196**, 375 (2013).
[45] X. Mo and Y.Yang, Sci China **48A**, 115 (2005).
[46] Q. He, F.-Q. Zeng, and D.-X. Zheng, Acta Math. Sci. **37B**, 1162 (2017).
[47] G. Randers, Phys. Rev. **59**, 195 (1941).
[48] C. Pfeifer and M. N. R. Wohlfarth, Phys. Rev. D **84**, 044039 (2011).
[49] R. Ruffini, J. Tiomno, and C. Vishveshwara, Lett. Nuovo Cimento **3**, 211 (1972).
[50] B. F. Schutz and C. M. Will, Astrophys. J. **291**, L33 (1985).
[51] S. Iyer and C. M. Will, Phys. Rev. D **35**, 3621 (1987); S. Iyer, Phys. Rev. D **35**, 3632 (1987).
[52] R. A. Konoplya, Phys. Rev. D **68**, 024018 (2003).
[53] M. Dafermos, G. Holzegel, and I. Rodnianski, Acta Math. **222**, 1 (2019).
[54] C. Gundlach, R. H. Price, and J. Pullin, Phys. Rev. D **49**, 883 (1994); **49**, 890 (1994).